Mass-Selective Chiral Analysis

Ulrich Boesl and Aras Kartouzian

Department of Chemistry, Technische Universität München, 85747 Garching, Germany; email: ulrich.boesl@tum.de, aras.kartouzian@tum.de

Annu. Rev. Anal. Chem. 2016. 9:343–64

First published online as a Review in Advance on April 6, 2016

The *Annual Review of Analytical Chemistry* is online at anchem.annualreviews.org

This article's doi: 10.1146/annurev-anchem-071015-041658

Keywords

circular dichroism, chirality, enantiomeric recognition, heterogeneous asymmetric catalysis, laser spectroscopy, mass spectrometry

Abstract

Three ways of realizing mass-selective chiral analysis are reviewed. The first is based on the formation of diastereomers that are of homo- and heterotype with respect to the enantiomers of involved chiral molecules. This way is quite well-established with numerous applications. The other two ways are more recent developments, both based on circular dichroism (CD). In one, conventional or nonlinear electronic CD is linked to mass spectrometry (MS) by resonance-enhanced multiphoton ionization. The other is based on CD in the angular distribution of photoelectrons, which is measured in combination with MS via photoion photoelectron coincidence. Among the many important applications of mass-selective chiral analysis, this review focuses on its use as an analytical tool for the development of heterogeneous enantioselective chemical catalysis. There exist other approaches to combine chiral analysis and mass-selective detection, such as chiral chromatography MS, which are not discussed here.

1. INTRODUCTION

Enantiomeric excess (ee): excess of one enantiomer over the other enantiomer in a mixture

Asymmetric catalysis: type of catalysis in which formation of one enantiomer is favored over the other

Circular dichroism (CD): the difference in absorption of left- and right-handed circularly polarized light

Diastereomers: strongly or weakly bound complexes of chiral molecules with the same (homo-) or opposite (hetero-) chirality

Photoelectrons: electrons emitted from molecules (surfaces) when photon energies (single or multiphoton absorption) exceed the ionization threshold (work function)

Since the discovery of the optical activity (the ability to rotate linearly polarized light) of asymmetric compounds in the beginning of the nineteenth century, chiral molecules have gained increasing interest in various fields of chemistry. One main reason for this interest is the different biological activity of two corresponding enantiomers and thus their importance in the pharmaceutical and food industries. Asymmetric synthesis, that is, the synthesis of one of the enantiomers in high enantiomeric excess (ee), is without doubt a major discipline in chemistry. In this regard, asymmetric catalysis is a key technology. The majority of asymmetric reactions at the moment employ homogeneous catalysts (1, 2). There is, however, a strong drive for heterogeneous asymmetric catalysis, which promises lower catalyst contamination, lower price, and higher turnover numbers (3). Heterogeneous asymmetric catalysis is not well understood, in part because chiral diagnostic techniques in the gas phase are not easily applied under well-controlled conditions (e.g., ultrahigh vacuum conditions and model systems). The ability to analyze the product(s) of a reaction using enantiosensitive methods under controlled conditions is a prerequisite for understanding the mechanisms involved and for the development of more efficient asymmetric catalysts. The low number of product molecules and the presence of mixtures in such experiments push the common enantioanalysis methods, such as circular dichroism (CD) and chromatography, beyond their applicability limits. As demonstrated in this review, sensitive and mass-selective chiral analytical tools are needed for such studies as well as for numerous other applications.

In the last three decades, three principal options to perform enantioselective mass spectrometry (MS) have been developed. In the first, described in Section 2, features of diastereomers are exploited to recognize the chirality of chemical substances. These features concern differences in fragmentation, formation, or spectroscopy of diastereomers containing the substance of interest and preselected enantiomers of chiral probe molecules. The second option (Section 3) involves the use of resonance-enhanced multiphoton ionization (REMPI) in the ion source of a mass spectrometer. Excitation to a higher electronic molecular state allows inclusion of ultraviolet (UV) spectroscopy in the control of the multiphoton ionization (MPI) process. Consequently, electronic circular dichroism (ECD) can be combined with MPI using circularly polarized light. The third option (Section 4) is also based on photoionization, but now the photoelectrons, the spatial angular distribution of which is resolved, carry the chiral information. The latter is not a mass-selective method per se. However, performing angle-resolved photoelectron spectroscopy (PES) in coincidence with the appearance of molecular ions of interest allows enantioselective MS. In Section 5, the three approaches are summarized and compared. Having asymmetric heterogeneous catalysis in mind as a major goal, we also include recent related activities regarding enantioanalysis and chiral diagnostic.

2. ENANTIOSENSITIVE MASS-SELECTIVE DETECTION BASED ON DIASTEREOMERS

MS is capable of rapid and reliable analysis of multicomponent mixtures based on the different molecular mass of each component. In its simplest form, MS is not able to distinguish among different molecules that have the same molecular mass. However, there are ways to overcome this shortcoming. In the case of different molecules, such as pentene (C_5H_{10}; 70 amu) and propylene aldehyde (C_4H_6O; 70 amu), the fragmentation pattern can be analyzed to tell the molecules apart. The same approach can be used in some cases to distinguish structural isomers (e.g., pentan-2-one and pentan-3-one).

In contrast to the examples above, enantiomers possess identical fragmentation patterns and thus cannot be identified in that way. Placing the sample in a chiral environment can, however,

make MS enantiosensitive based on the enantioselective intermolecular interactions of a "host" enantiopure molecule with the enantiomers of "guest" chiral molecules. In such an approach, the host-guest diastereomers possess different fragmentation patterns, formation kinetics, chemical reactivity, and spectroscopical properties, which depend on the handedness of the components. In 1977, Fales & Wright (4) demonstrated the difference in ion intensities for dimers of isotopically labeled dimethyl-d_6 D-tartrate and dimethyl-d_0 L-tartrate, using chemical ionization MS. They observed a pronounced deviation from the expected signal ratio of 1:2:1 for d_6-d_6, d_6-d_0, and d_0-d_0 dimers in the racemic sample, disfavoring the formation of heterochiral dimers.

Approximately a decade later, Baldwin et al. (5) performed similar experiments on isotopically labeled D- and L-diisopropyl tartrate using fast atom bombardment mass spectrometry (FABMS) and could confirm the favored formation of homochiral dimers. In these early works, mass spectrometric chiral recognition was facilitated by isotopic labeling, which requires advance knowledge of the components' handedness. As the main goal of such experiments is to determine the ee of a chiral compound with an unknown enantiomeric purity, such approaches are not suitable. Nonetheless, these studies showed the potential of a host-guest approach for chiral recognition based on diastereomeric effects. In this section, the different approaches to enantiosensitive gas phase MS based on diastereomeric effects and without isotopic labeling of guest molecules are summarized and some examples are given.

2.1. Relative Abundance of Homo- and Hetero-Diastereomers

Sawada et al. (6) used the diastereomeric effect to determine the enantioselectivity of FABMS by introducing the relative peak intensity (RPI) method. In RPI, an equimolar amount of an achiral reference host molecule is added to the chiral target host before complexation with the chiral guest compound. The RPI value of two resulting complex ions (chiral host-guest and reference host-guest) in a single mass spectrum is then determined. This measurement is performed for both enantiomers of the guest compound. Once the RPI is known for both enantiomers, the ee of an unknown mixture can be determined. The RPI method is illustrated in **Figure 1*a***. To be able to determine the ee of chiral compounds while benefiting from isotopic labeling, one could use an equimolar mixture of host enantiomers, one of which is isotopically labeled. This concept is illustrated in **Figure 1*b***. Sawada et al. (7) used such an enantiomer-labeled host method to determine the ee of phenylglycine methyl ester hydrochloride enantiomeric mixtures (guest compound) by FABMS. This method has been applied to a range of systems ever since for ee determination and chiral recognition (8–14). A number of related reviews have also dealt with this topic recently (15–17).

2.2. Kinetics of Diastereomers' Fragmentation

Kinetic methods: methods that allow determination of heat of formation of molecular fragments by mass spectrometry, enabling differentiation of hetero- and homo-diastereomers

The first demonstration of enantiomeric recognition using kinetic methods was reported by Vékey & Czira (18). Building upon the kinetic method developed by Cooks & Kruger (19), commonly used for determination of thermochemical values, they looked at fragmentation kinetics of protonated trimers of the type A_2BH^+, where A and B are chiral compounds and the handedness of one of them is known. In this approach, fragmentation in four competitive channels, either caused by autofragmentation of metastable complexes or as a result of collision-induced dissociation, is compared (**Figure 2**). The differences in gas phase basicity of the dimers are utilized to determine the handedness of the unknown chiral compound by determining whether the fragmented dimer is homo- or heterochiral. Vékey & Czira (18) showed that for five different pairs of amino acids, differences as small as 0.2 kJ/mol in gas phase basicity of homochiral and heterochiral dimers can

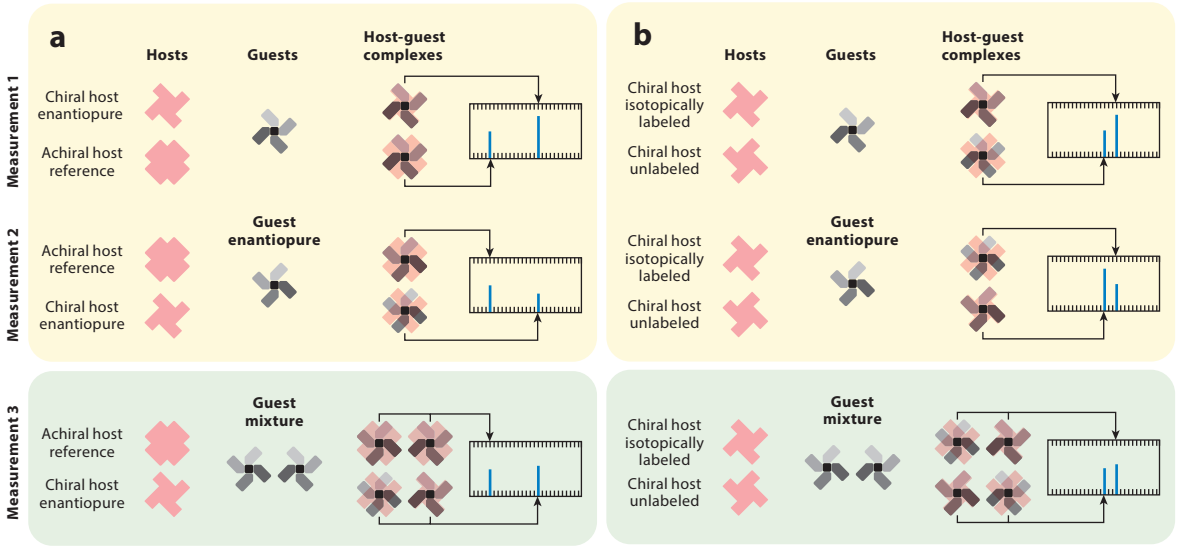

Figure 1

(*a*) Dimers of a chiral guest molecule with a chiral/achiral mixture as the host are measured using mass spectrometry (MS) (measurement 1). The mass separation is achieved due to the different masses of the chiral and achiral host molecules. The same measurement is then repeated for the other enantiomer of the guest molecule (measurement 2). In both cases, the complexes with the achiral host should show the same intensity, but the complexes with the chiral host molecules will show different intensities reflecting the stability of homo- and hetero-diastereomers. Thus, the enantiomeric excess (ee) of a mixture of the guest molecules can be determined (measurement 3). (*b*) Dimers of an equimolar mixture of a chiral host molecule, where one of the enantiomers is isotopically labeled, and a chiral guest molecule are studied using MS (measurement 1). The mass separation is achieved due to the isotopically induced mass difference between the two enantiomers of the host molecule. The same measurement is then repeated for the other enantiomer of the guest molecule (measurement 2). These two measurements clearly show the affinity of the chiral guest to form either homo- or hetero-diastereomers with the host molecule. The ee of an unknown mixture of the guest molecule can thus be determined as depicted in measurement 3.

be reliably measured. Soon after, Cooks and coworkers also applied the method for chiral discrimination of amino acids using the dissociation kinetics of copper(II) (20) and Ni(II) (21) complexes. Many systems have been studied by the kinetic method in the past (22–25). The method was improved further by Young & Cooks (26) in terms of its lack of reliability in chiral selectivity of samples with high ee (above 90%). Other extensions to the original kinetic method have since been developed to expand its applicability under more diverse conditions (27–30).

2.3. Spectroscopy of Homo- and Hetero-Diastereomers

The first example of spectroscopic chiral discrimination in the gas phase using the diastereomeric effect was reported by Zehnacker and coworkers (31). They showed that the diastereomeric complexes between enantiomers of α-methyl-2-naphthalenemethanol and a chiral alcohol (2-chloro-1-propanol) possess different excitation spectra. Although this study did not utilize MS, it paved the way for mass spectrometric approaches based on different spectroscopic properties of homo- and heterochiral diastereomers.

Speranza and coworkers (32) were the first who took advantage of this effect while combining REMPI and time-of-flight (TOF) to look at the vibronic spectra of molecular complexes between (R)-(+)-1-phenyl-1-propanol and enantiomers of 2-butanol. They showed that differences in photoionization fragmentation pattern and bathochromic shifts of the electronic band origin

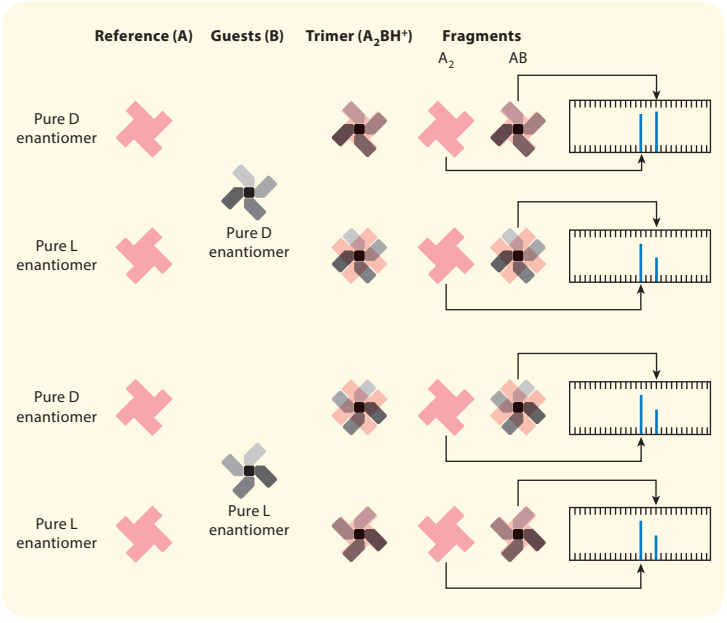

Figure 2

Trimers of two enantiopure chiral molecules of the form A_2B studied mass spectrometrically for dissociation/fragmentation of dimers (either A_2 or AB). The experiment is performed for all four combinations (two enantiomers of A and B lead to four sets of A_2B trimers). Whereas A_2 is always a homochiral dimer and thus serves as a reference, AB can be either homo- or heterochiral. The mass separation is achieved due to the mass difference of A and B units. Abbreviations: D, dextrorotatory; L, levorotatory.

relative to that of the pure chromophore can be used for chiral recognition. This approach has been used for enantiodifferentiation of various molecular complexes in the gas phase (33–44).

3. ENANTIOSENSITIVE MASS-SELECTIVE DETECTION ON THE BASIS OF CIRCULAR DICHROISM IN PHOTOABSORPTION

The second option for enantiosensitive MS is based on UV spectroscopy with circularly polarized light, or ECD (45). It can be realized by combining either (*a*) spectroscopy and ionization, as in REMPI (46), or (*b*) spectroscopy and dissociation, as in multiphoton absorption (47), predissociation applied to molecular ions (48), or neutral molecules (49). REMPI consists of absorption via resonant intermediate states of a molecule up to its ionization continuum. The first absorption step usually is the same as in conventional UV spectroscopy. In this case, the ion yield is controlled by the UV spectrum of the ionized molecule (46). The benefits of REMPI combined with MS (preferably TOF MS) are chemically selective ion formation, sensitivity, and speed. Numerous analytical applications of REMPI have been published, such as for sub-ppt (parts per trillion) analysis of aromatics in water (50), ionization in atmospheric pressure ion sources (51), trace analysis in automotive exhaust gases (52, 53), or selective ionization of molecules desorbed from single particles in an online aerosol mass spectrometer (54), just to name a few (for a review, see 55 and references in 46, 50–55). In this section, experimental setups and results for the spectroscopy and ionization approach to enantiosensitive MS are presented. The combined spectroscopy and dissociation approach has not yet been realized experimentally, but may provide further interesting features for enantiosensitive MS.

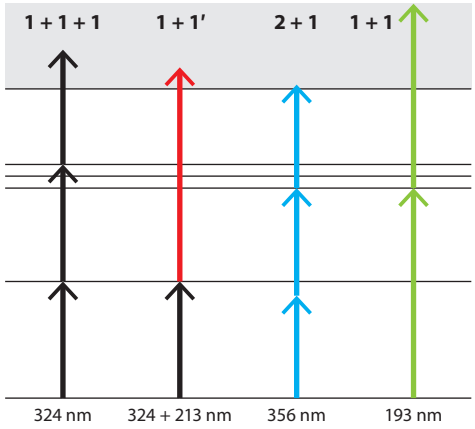

Figure 3

Various multiphoton excitation schemes using the example of 3-methylcyclopentanone.

The first experiments in which REMPI, CD spectroscopy, and MS have been combined were published by Compton and coworkers (56). They used (2+1)-REMPI with 200 nm photons to excite the chiral molecule 3-methylcyclopentanone (3-MCP) via the lowest Rydberg state 3s and ionized it by absorption of a third photon. In this case, the resonant intermediate state was excited by two-photon absorption and thus nonlinear two-photon spectroscopy (57, 58) was relevant. CD of two-photon spectroscopy was already the subject of theoretical studies (59–63). Shortly after Compton's work, Boesl and coworkers (64, 65) ionized the same molecule with 324 nm laser light via (1+1+1)-REMPI, where conventional one-photon UV spectroscopy and ECD, respectively, of the $n\pi^*$ transition of 3-MCP were involved. All these processes are based on multiphoton absorption beyond the ionization threshold whereby one or more resonant intermediate states are excited through the integration of spectroscopy and CD in the process of photoionization. In **Figure 3**, exemplary absorption processes are presented together with laser wavelengths for REMPI of 3-MCP.

In both experiments cited above, nanosecond lasers were used. Weitzel and coworkers (66–69) and Baumert and coworkers (70) applied femtosecond lasers with circularly polarized emission inducing MPI processes of higher order (800 nm photons) to study CD effects on molecular and fragment ions. Molecules such as 3-MCP (66), limonene (70), and propylene oxide (69) have been studied. A considerably reduced fragmentation rate with respect to nanosecond excitation was found as well as interesting differences in the CD effect monitored via molecular and fragment ions (69, 70). These also showed up in the nanosecond studies as discussed below (71–75). Comparison of femto- and nanosecond experiments may help to detect and study fast intramolecular rearrangement processes resulting in a change of CD or even disappearance of chirality.

In the following, the experimental setup used by the group of Loge & Boesl (76) is described (**Figure 4**). The experiment includes a wavelength-tunable laser, an Nd:YAG (neodymium-doped yttrium aluminium garnet) laser–pumped frequency-doubled dye laser, emitting in the wavelength range of 300 to 340 nm. A quarterwave retardation plate is used to achieve circularly polarized light. Its rotation by 90° results in a change from left- to right-handed polarization and vice versa. Circularly polarized light is focused into the effusive molecular beam of a small TOF mass spectrometer. This beam originates from a capillary that is coaxial with the axis of the TOF ion optics, which consists of three centrosymmetric electrodes with holes in the middle for ions to

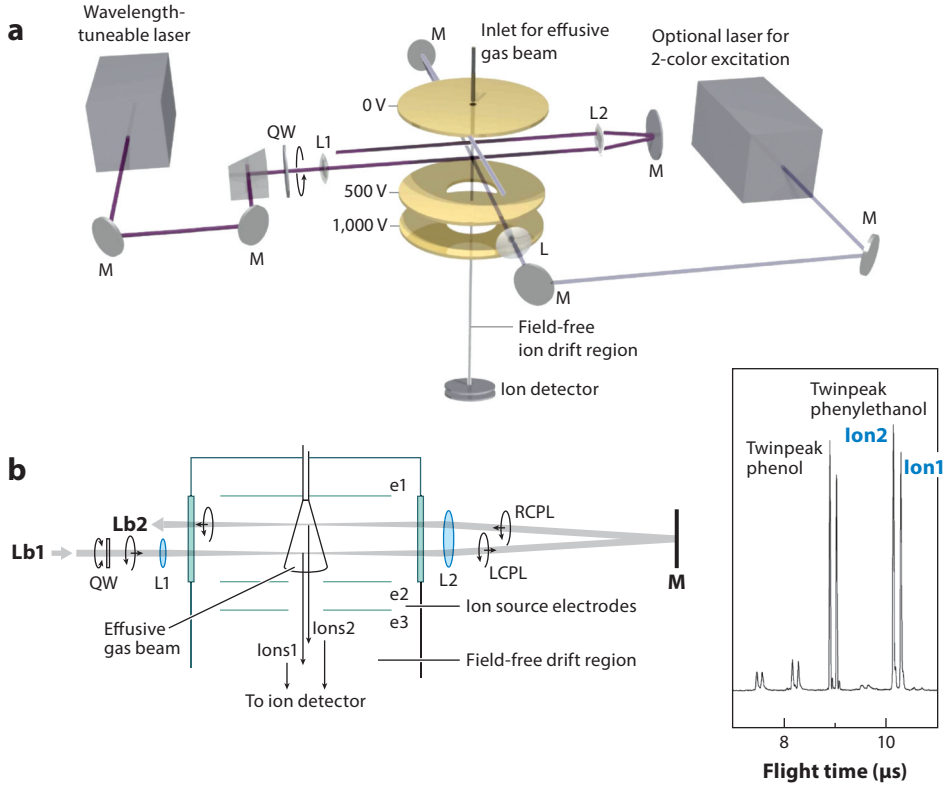

Figure 4

(*a*) Experimental setup of CD-LAMS via REMPI ionization. Reproduced with permission from Reference 133. Copyright 2009, Springer. (*b*) Arrangement for reflection of laser beam 1 (Lb1) with intrinsic switch of circular polarization and twin peak mass spectrometry and an exemplary mass spectrum of phenylethanol (chiral) and phenol (achiral). Reproduced with permission from Reference 71. Abbreviations: CD-LAMS, circular dichroism laser mass spectrometry; e1–e3, electrodes of the ion optics; L1–L2, lenses; LCPL, left circularly polarized laser; M, mirrors; QW, rotatable quarterwave plate for left- or right-handed circular polarization; RCPL, right circularly polarized laser; REMPI, resonance-enhanced multiphoton ionization.

pass. High voltages are applied to accelerate the ions out of the ion source into the field-free drift region where ions of different masses are separated. The disadvantage of a three-photon process, such as (1+1+1)-REMPI, is that fairly large laser pulse energies are needed for sufficient rates of ionization. This can be circumvented by two-color excitation (**Figure 3**) where a second linearly polarized laser with 213 nm (fifth harmonic of an Nd:YAG laser) is focused into the small overlap volume of the first laser beam and the molecular beam. **Figure 4** shows that the first laser beam is reflected back into the effusive gas beam. This is one of several measures to cope with the problem of pulse-to-pulse fluctuations of laser power. The goal of this two-beam approach for the primary laser is to get ion signals for left- and right-handed polarized light from every single laser shot (75). If a second laser beam is used for two-color excitation, it has to be reflected into the vacuum chamber where the molecular beam and primary reflected beam are overlapping. The arrangement of back reflection is displayed in **Figure 4*b*** and described below.

Laser beam (Lb)1 in **Figure 4** is focused into the molecular beam, induces (1+1+1)-REMPI, passes the vacuum chamber and a parallelizing second lens L2, and is reflected by mirror M.

Circular polarization: polarization of light (right or left circular) whose electric field vector is rotating clockwise or counterclockwise with respect to its direction of propagation

Because reflection turns the direction of propagation of light by 180° but does not change the direction of rotation of the electric field vector of circularly polarized light, the sense of circular polarization is switched from left- to right-handed, or vice versa. This two-beam approach allows ion signals for left- and right-handed circularly polarized light to be obtained simultaneously for every single laser pulse. As the asymmetry factor g is the relative difference of ion currents, it does not depend on laser pulse fluctuations, at least in first order. To observe ion current I2 from laser beam Lb2, the latter is refocused into the molecular beam by lens L2. The next task is to separate ions from beams Lb1 and Lb2 in the mass spectrum. This is done by an ion optical trick (75). Usually, one runs a linear TOF mass spectrometer so that the space focus, a point of ion cloud compression and thus of enlarged mass resolution, lies on the surface of the ion detector (77). Under certain conditions, a second-order space focus correction with enhanced mass resolution is achievable (78, 79), which shows up in the flight time–to–position curve as a flat turning point, meaning that ions formed in a large range between positions a and b in the ion source arrive at the ion detector simultaneously. Here, however, separation of ions formed at positions a and b is the goal. To reach this, the flight time–to–position relation is detuned, changing the turning point into a minimum (position a) and a maximum (position b) that do not represent space foci of second, but still of first order. Flight times from positions a and b now are quite different, with corresponding mass peaks well separated. The detuning is achieved by slightly changing the intermediate electrode voltage. In **Figure 4**, the resultant mass spectrum of the chiral molecule phenylethanol is shown as an example. Two different ion peaks appear at a flight time of approximately 11 μs. Double mass peaks also are observed for fragment ions and phenol. This is used as an achiral reference substance that shows similar spectral features to phenylethanol due to a common aromatic ring (76). Differences of double peaks from achiral ions are artificial effects and used to correct CD effects of chiral substances.

In summary, from beam reflection and twin mass peaks we obtain ion currents I1 and I2 for each single laser pulse, where I1 is due to left and I2 to right circularly polarized light. Following the formula for the asymmetry factor,

$$g_{REMPI} = \Delta\varepsilon/\varepsilon = (\varepsilon^L - \varepsilon^R)/\varepsilon = \Delta I/I = \frac{1}{2}(I^L - I^R)/(I^L + I^R), \quad 1.$$

which describes the relative difference of extinction coefficients or ion signals from left- (L) and right (R)-handed circular polarization excitation, we obtain an experimental g-value of the sample molecule. Similarly, an artificial g-value for the achiral reference from the same mass spectrum is obtained. Subtracting this from the experimental sample value gives a corrected g-value:

$$g_{corr} = g(\text{sample})_{exp} - g(\text{reference})_{exp}, \quad 2.$$

where exp indicates measured values being subject to systematic errors. Because artificial asymmetry may be induced by laser beam 1 being left- and laser beam 2 right-handed polarized, the polarization of incoming beam 1 then is changed to right-handed circular polarization with laser beam 2 automatically being left-handed polarized. The average gives the final g-value:

$$g = \frac{1}{2}(g^{LR} - g^{RL}) \quad 3.$$

with $g^{RL} = 1/2\ (I^R - I^L)/(I^L + I^R)$. This is repeated for several hundred laser pulses resulting in an average value for one measurement cycle. These are repeated some 20 to 30 times. Using a laser with 30 Hz repetition rate, it takes 1–5 min to get a final mass-resolved asymmetry factor.

This method has been applied to different molecules, including several carbonyls, molecules with aromatic ring systems, or substances such as pinene or limonene (80). In some cases, for example, limonene, even conventional CD measurements in the gas phase are available from the literature. The value of $g = -0.13\%/213$ nm (81) compares well with $-(0.16 \pm 0.06)\%/213$ nm

(80) from CD-REMPI. Even some solvent values show similarities with REMPI gas phase measurements. Thus, S-phenylethanol exhibits a decrease of the CD effect from +0.63% to +0.26% for a change of exciting wavelength from 266 nm to 260 nm, which compares well to a decrease from +0.2% to +0.1% in aqueous solution at the same wavelengths (82–84).

3.1. Double-Resonance Circular Dichroism

All of the results mentioned above (although performed mass selectively) can be compared with conventional CD with one exception: the (1+1+1)-REMPI of 3-MCP (80). The double resonance CD (**Figure 3**) induces an enhancement of the CD from 0.20 to 0.27, an effect that is not possible with conventional CD spectroscopy. This is already an indication that CD-REMPI MS allows for completely new experiments that are not possible with conventional CD. In the following sections, three such new options for CD spectroscopy are presented.

3.2. Two-Photon Circular Dichroism

In two-photon CD (72), the first electronic transition is excited by two- instead of one-photon absorption. Two-photon spectroscopy is a nonlinear phenomenon (comparable to Raman spectroscopy). There is extensive theoretical work on two-photon CD (59–63, 85) but a vanishingly small number of experimental results. There are, however, interesting aspects to be considered. (*a*) The vacuum ultraviolet (VUV) spectral range (<200 nm) is accessible with visible or near-UV light. (*b*) Two-photon absorption is subject to different, often opposite selection rules, allowing access to electronic states with different symmetry (e.g., the $3p_x$ Rydberg state shown in **Figure 5**). (*c*) In some cases, enhancement of the CD upon two-photon excitation is expected. (*d*) Two photons allow different combinations of photon polarizations, and three of them are independent. The question of whether this allows determining the handedness of chiral molecules without extensive theoretical calculations has been discussed (59).

At the bottom of **Figure 5**, the one-photon VUV value of an early work (86) taken in the energy range of low molecular Rydberg states of 3-MCP is displayed. The g-values are in the low and sub-ppm range. Two of these values (for the vibrationless 3s-Rydberg state and for the 3s state with one quantum of vibration 6 excited) are verified by (1+1+1)-CD-REMPI using a frequency-doubled dye laser (71). **Figure 5** also displays two-photon values. The photon energy is now half of the VUV photons. The pioneers who observed two-photon CD effects in the isolated gas phase were Compton and coworkers (56). They determined a two-photon g-value of the transition to the 3s-Rydberg state of 1.5%, which is a sevenfold enhancement compared with one-photon CD. Logé & Boesl (71) could verify this value and, in addition, found comparable g-values for the $3p_y$ and $3p_z$ Rydberg states by CD-REMPI monitored via the molecular ion (*m/z* 98). Again, enhancement with respect to one-photon CD is observed in addition to a change of sign. Because CD-REMPI can be performed mass selectively, g-values can also be monitored via fragment ions. Doing this, an astonishing increase of the g-value by a further factor of five to ten is found, although with opposite sign. One explanation is that this is an effect of consecutive absorption in the molecular ion.

3.3. Molecular Ion Circular Dichroism

In the experiment depicted in **Figure 5**, the CD effects of neutral and ionized molecule are mixed. They can be disentangled by measuring the effect in the molecular ion (only neutral CD) as well as in the fragment ion peak (71, 72) (includes absorption in the molecular ion). To capture more information, laser pulse energies were varied. Although the g-values measured via the molecular

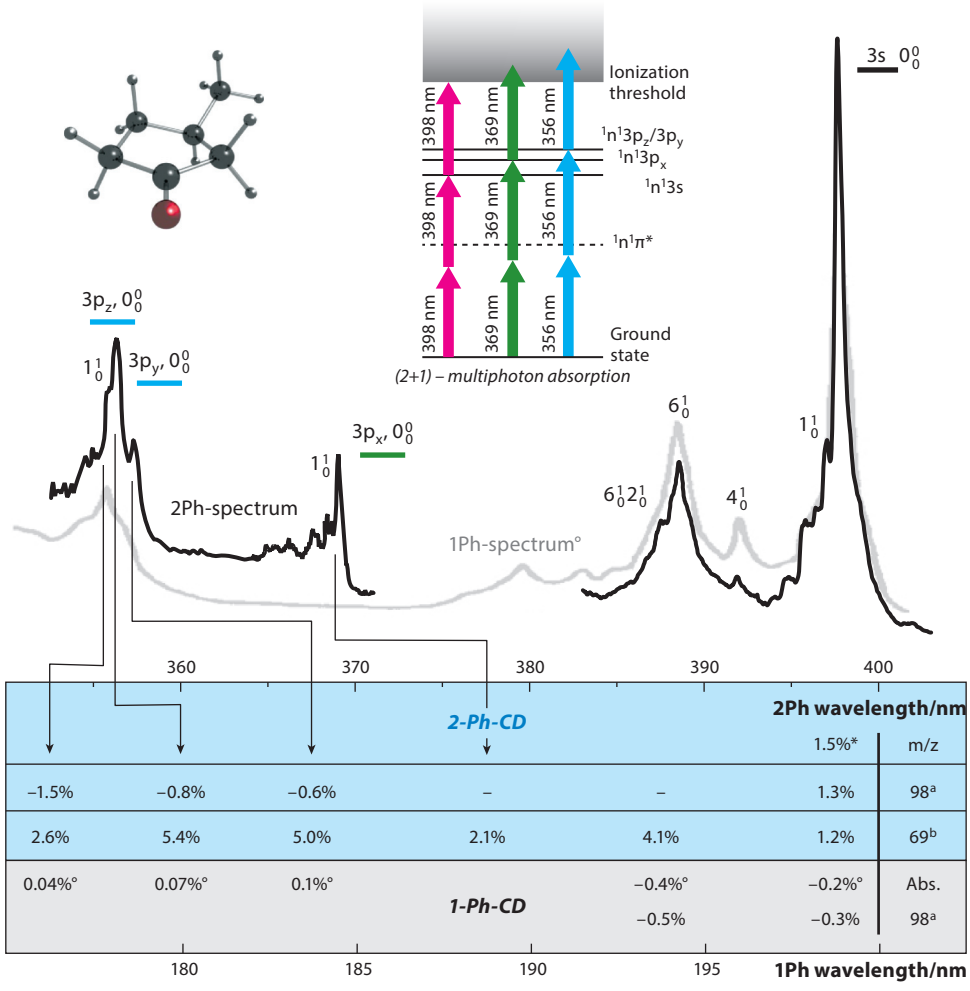

Figure 5

Two- (2 Ph) and one-photon (1 Ph) spectra of 3-MCP with CD values for both types of photoexcitation. Shown in the bottom panel are [a]CD-REMPI monitored via molecular ion mass peak *m/z* 98; [b]CD-REMPI monitored via fragment ion mass peak *m/z* 69; *CD-REMPI monitored via total ion current and separately via electron current (56); and °CD-VUV absorption (Abs.) spectrum (81). Two-photon values are displayed in blue. Some of the vibrational modes (1–6) excited in the resonant intermediate state are also depicted in the top panel: 1, ring out-of-plane bending mode; 2, ring twist mode; 3, methyl torsion mode; 4, CO-in-plane bending mode; 5, ring in-plane bending mode; and 6, CO stretching mode. Rydberg states are indicated by 3s, 3px, 3py, and 3pz. Reproduced with permission from Reference 71. Abbreviations: CD-REMPI, circular dichroism–resonance-enhanced multiphoton ionization; CD-VUV, circular dichroism–vacuum ultraviolet; MCP, 3-methylcyclopentanone.

ion peak did not show significant dependence on laser intensity, strong dependence of the CD effect monitored via the fragment ion was found as shown in **Figure 6**. The decrease of the g-values with increasing laser intensity above 2 mJ/pulse is easily explained. With increasingly stronger absorption, differences of absorption get weaker and weaker due to absorption saturation. The strong decrease for small laser intensities, however, is surprising. A plausible explanation is offered by fast

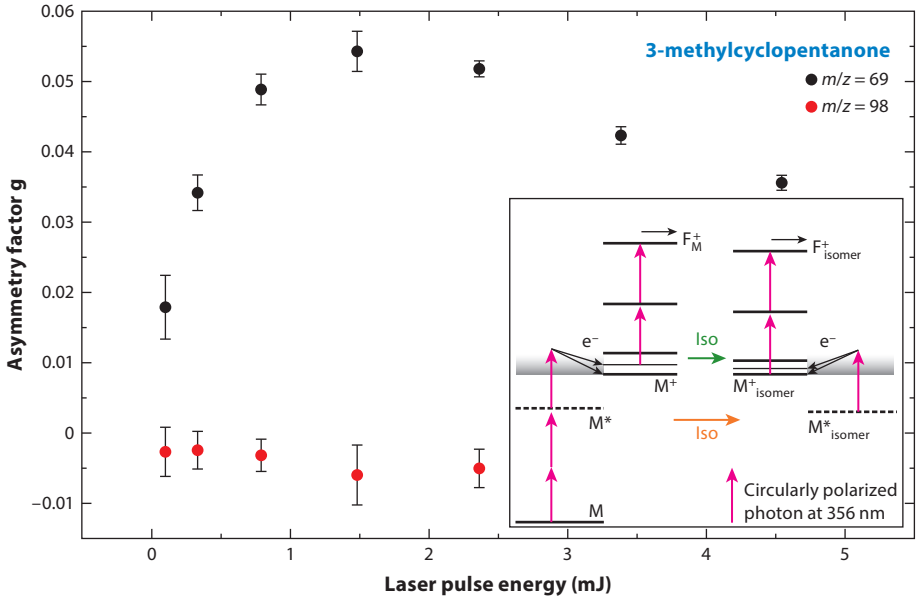

Figure 6

(2+1)-CD-REMPI of 3-MCP at 356 nm monitored via molecular ion and a fragment ion signal. The laser power has been varied from 0.1 to 4.5 mJ/pulse, revealing a CD effect in the molecular ion. (*Inset*) Explanation of the varying CD effect with laser power. At low laser power, isomerization of the molecular ion (*green arrow*) or the excited neutral molecule (*orange arrow*) may result in achiral isomer structures (e.g., due to ring opening). Different CD of molecular and fragment ions was also observed for limonene (70) and propylene oxide (69) in femtosecond laser experiments. Reproduced with permission from Reference 72. Abbreviations: CD, circular dichroism; CD-REMPI, circular dichroism–resonance-enhanced multiphoton ionization; iso, isomerization; MCP, methylcyclopentanone.

intramolecular processes resulting in achiral molecular structures (e.g., by ring opening) without changing the molecular mass (no fragmentation). As depicted in **Figure 6**, these fast processes may take place in the ionic ground state or in highly excited neutral states of the molecule. They will dominate at small laser pulse intensity (small photon density) corresponding to large time gaps between consecutive absorption steps but be inactive at high intensities or fast excitation. This is supported by the femtosecond-laser mass spectrometry experiments of Baumert and coworkers (70) and Weitzel and coworkers (69) who observed similar effects for limonene (70) and propyleneoxide (69). **Figures 5** and **6** (performed with nanosecond lasers) indicate these processes take place on the subnanosecond timescale. Whether the ionic or neutral relaxation channel is active is not yet clear. Pump-probe experiments (72) with delayed laser pulses revealed a vanishing molecular ion CD effect supporting the ionic channel model, whereas theoretical work by Kröner and colleagues (73, 74) presumed that the chiral molecular structure was rather stable. No molecular ion CD effect is found for the 3s-Rydberg state as opposed to the more energetic 3p-Rydberg states (**Figure 5**). One explanation could be that unstable excited ionic states are populated at REMPI via 3p-Rydberg states. The neutral decay channel model is not supported by the experimental results. Nevertheless, the experiments in **Figures 5** and **6** prove that molecular ion CD spectroscopy is possible by CD-REMPI. This may be used to study fast dynamic molecular processes where pure spectroscopy or MS do not work or to probe the chirality of large involatile organic molecular ions brought into the gas phase by matrix-assisted laser desorption/ionization (MALDI).

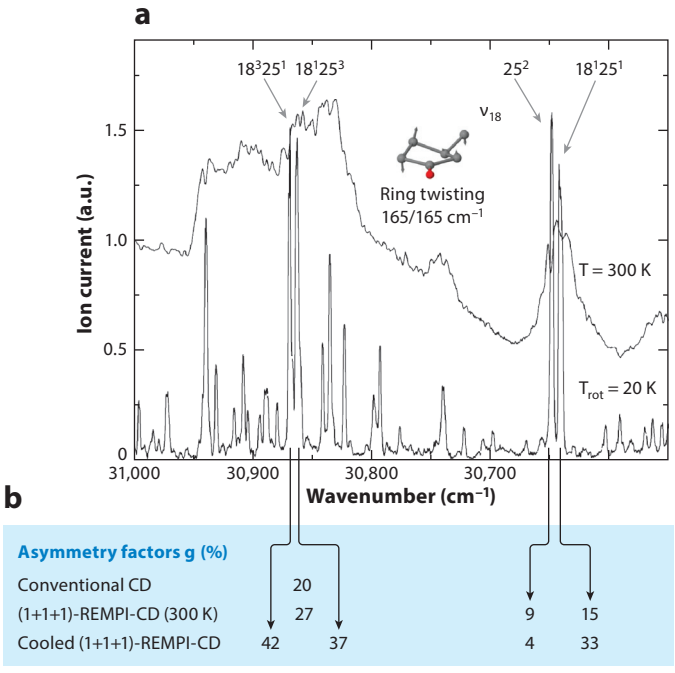

Figure 7

(*a*) Room temperature (300 K) and supersonic beam–cooled (20 K) spectra of 3-MCP measured via (1+1+1)-REMPI with tentative assignment of vibronic transitions. (*b*) Asymmetry factors g for four vibronic bands selectively excited in the cold spectrum. In the warm spectrum, the bands $18^3 25^1$ and $18^1 25^3$ are fully overlapping (only one g-value is given). (*Inset*) Structure and ground/excited state frequency of the ring twisting mode 18, which is supposed to enhance the electronic CD effect. Mode 25 is the CO-out-of-plane bending vibration. Superscripts indicate the number of excited vibrational quanta. Reproduced with permission from Reference 87.

3.4. Cold-Molecule Circular Dichroism

The third CD-REMPI experiment presented here discusses the use of mass-selective laser-CD spectroscopy on molecules cooled in a supersonic beam (87). This allows excitation of single vibronic bands. Supersonic beam cooling is well known and well introduced in molecular spectroscopy (88–92). Two research groups performed CD measurements of supersonic beam–cooled molecules (56, 93) to discriminate unwanted conformers by spectroscopic means. The goal of the experiment presented here was to study the influence of single isolated vibrations on the ECD effect and find CD-promoting vibrational modes. Two problems appeared: The twin peak method could not be applied due to geometrical reasons, but a subsequent redesign is feasible. The achiral reference method was problematic because line narrowing by molecular cooling did not allow accidental band overlap of analyte and reference molecules. To enable the overlap, an in-line effusive gas beam (**Figure 3**) was used that intersected the cold beam at the point of laser ionization. This also allowed comparison of warm and cold spectra and CD effects.

Supersonic beam: molecular beam formed upon gas expansion into vacuum reveals velocity distributions and internal motions of molecules cooled far below room temperature

In **Figure 7**, the room temperature spectrum and cold spectrum of the nπ* transition of 3-MCP around 325 nm is displayed. Strong line narrowing is achieved by cooling rotational and low-frequency vibrational molecular motions. In the warm effusive beam, low-frequency vibrations cause many hot bands that congest the spectrum. A tentative assignment of the four major vibronic bands in **Figure 7** is given following the vibrational assignment of cyclopentanone (94). In the

selected wavelength range, mainly the ring-bending mode 25 (folding around the CO axis) and the ring-twisting mode 18 (twisting around the CO axis) determine the spectrum. CD measurements at these four vibronic bands in the effusive beam supply (1+1+1)-CD-REMPI values of 27% (20% conventional CD) near 30,850 cm^{-1} and 9% and 15% around 30,650 cm^{-1}. In comparison, an enhancement in the cold spectrum of up to a factor of 2 for three of the four bands is found. Only the band assigned as 25^2 reveals a considerably smaller g-value in the cold spectrum. It seems quite obvious that in the effusive beam, the overlap of many bands levels out the large but also the small g-factors. It also seems that mode 18 has a CD-enhancing effect. A plausible explanation could be that the twisting of the ring leads to a rotation of the electron distribution in the π-orbital system of the carbonyl group. Rotation of an electron distribution will induce a momentary magnetic dipole moment along the axis of rotation (here, the CO axis). Classical models describe CD as cooperation of magnetic and electric transition moment, which is particularly favorable in carbonyls such as 3-MCP. Of course, this illustrative view has to be consolidated theoretically. Up to now, the influence of vibrations on ECD has been underestimated by theory (95–97). From an analytical point of view, it may help to enhance CD effects and thus sensitivity in mass-selective CD-REMPI.

Photoion: molecular cation formed when photon energies exceed the molecular ionization threshold supplied to the molecule by single or multiphoton absorption

4. ENANTIOSENSITIVE MASS-SELECTIVE DETECTION ON THE BASIS OF CIRCULAR DICHROISM IN PHOTOELECTRON EMISSION

In 1976, a novel chiral effect in the angle-resolved photoelectron emission of enantiomers was found theoretically (98). Further calculations predicted an exceptionally large CD effect in the order of 10% (99), which is two to three orders of magnitude larger than in conventional CD spectroscopy. Because molecular ionization thresholds are 8–12 eV, VUV photons are needed for one-photon ionization. This is the reason that the first relevant experiments have been performed at synchrotron facilities (100–102). Usually, the angular distribution of photoelectrons is recorded with spatially resolving two-dimensional electron detectors; therefore, this type of spectroscopy is also called imaging PES. If circularly polarized light is used, imaging photoelectron circular dichroism (PECD) may be observed. During the last decade, several chiral molecules have been characterized by this method (103–105). Recently, instead of synchrotrons, femtosecond lasers have been used (106, 107). This allowed the reduction of PECD from a large-scale to a table-top experiment (as in the other two methods described in Sections 2 and 3), making this method an interesting analytical tool. PECD is convincing because of its exceptionally high sensitivity for ee due to large CD effects, but it does not supply mass selectivity. This came into play through a very recent development where PECD was combined with photoelectron photoion coincidence (PEPICO) spectroscopy.

PEPICO is the combination of PES with photoionization MS (108). It is achieved by recording single photoelectron/photoion pairs in a TOF setup. Electrons are faster than ions by several orders of magnitude and therefore may serve as a trigger to measure the flight time of the corresponding ion from the event of photoionization to the arrival at the ion detector of a TOF mass analyzer. To avoid interferences of several photoionization events, the ionization rate has to be in the order of or smaller than the reciprocal ion flight time. One major application of PEPICO is preparation of molecular cations with well-defined internal energy due to:

$$E_{h\nu} = E_{IP} + E_{ion\text{-}int} + E_{el\text{-}kE} \qquad 4.$$

with ionizing photon energy $E_{h\nu}$, ionization potential E_{IP}, ion internal energy $E_{ion\text{-}int}$, and electron kinetic energy $E_{el\text{-}kE}$. PEPICO also allows for detecting the appearance of fragment ions and dissociation thresholds, respectively, and thus supplies access to the thermochemistry of the sample molecules. The first PEPICO studies were performed by Brehm & von Puttkamer (109) on methane in 1967. In these and other early experiments, retarding grids or hemispherical energy

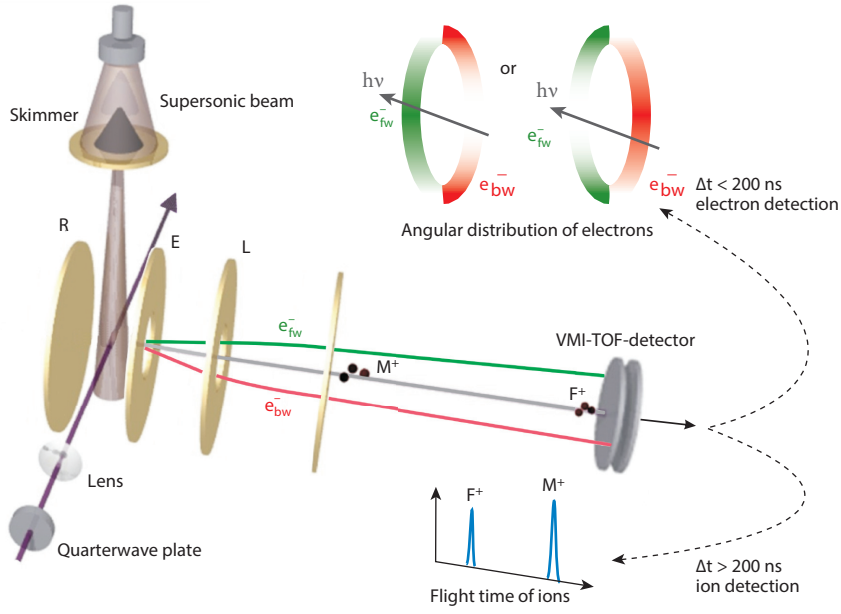

Figure 8

Single detector setup for a photoelectron circular dichroism (PECD) experiment with photoelectron photoion coincidence (PEPICO) detection using velocity map imaging combined with time-of-flight mass analysis (VMI-TOF) (113, 115, 116). The photoelectron number density reveals an asymmetry in forward (*green*) and backward (*red*) directions with respect to photon propagation (*violet arrow*) if circularly polarized light is used and one enantiomer of a chiral molecule is ionized. Switching the sense of circular polarization or changing the enantiomers results in an inversion of this asymmetry (as indicated by the two angular distributions of electrons at the *top* of the figure). 200 ns after electron detection, the voltages at the electrodes R (repeller), E (extractor), and L (ion optical lens) are switched and the molecular (M+) or fragment ion (F+) of the single primary electron/ion pair is extracted, giving rise to a TOF mass spectrum.

analyzers were used for electron detection and record-of-mass spectra as the use of photoelectron energy became possible. In modern PEPICO experiments, electron kinetic energy is monitored by velocity map imaging using very short duration light sources (e.g., femtosecond lasers) and has been pioneered by Hayden and coworkers (110–113). In 2008, a full double velocity image mapping coincidence spectrometer for femtosecond chemical dynamics was constructed (114).

In 2011, Janssen and coworkers (115) proposed PEPICO with circularly polarized femtosecond-laser light to achieve mass-selective PECD. Shortly after this work, Janssen and coworkers (116, 117) realized this approach by its application to camphor. Perspectives on this new promising method of mass-selective PECD are discussed by Janssen & Powis (118). In the following, a special experimental setup described by Janssen and coworkers (116, 119) is examined, which makes PEPICO-PECD even more appropriate for table-top instrumentation. They use a single-detector coincidence setup with only one position- and time-sensitive particle detector for both electron and ion coincidence detection (**Figure 8**). Consequently, only one TOF analyzer is used, which works in a pulsed mode to analyze both species. The total length of the TOF analyzer, which is optimized for electron imaging, is only 11 cm from the interaction region to the detector. The field-free drift region is as short as 5.25 cm but nevertheless supplies a maximum mass resolution of $R_{FWHM} = 950$ for atoms. This can be explained by the low ionization yield of only one ion/electron pair per laser pulse (vanishing space charge effects; 77, 78), the short ion

formation time, and the fast particle detection electronics with very high temporal resolution. The electrodes R, E, and L are used in pulsed mode to extract the electrons and ions toward the detector (**Figure 8**). At step one of a measurement cycle, appropriate voltages for electron velocity map imaging are applied to these electrodes. At step two, approximately 200 ns after the ionizing laser pulse, the voltages on all three lenses are switched to voltages with opposite sign appropriate for ion extraction. At step three, approximately 20 μs after the ionization laser pulse, the voltages are switched back to the electron analyzing mode. This is repeated with a rate of 1 kHz.

Similar to the asymmetry factor g in conventional ECD spectroscopy and g_{REMPI} (Equation 1) in mass-selective laser ionization CD spectroscopy, an asymmetry factor $g_{MP-PECD}$ can be formulated for multiphoton (MP)-PECD (116, 118) and PECD-PEPICO, respectively. Difference in absorption ($\Delta\varepsilon/\varepsilon$ for single-photon excitation) is now replaced by difference in forward/backward ejection of electrons between left- and right-handed excitation:

$$g_{MP\text{-}PECD} = (I^{L,f} - I^{R,f})/0.5 - (I^{L,b} - I^{R,b})/0.5 \qquad 5.$$

Here, $I^{L,f}$ and $I^{R,f}$ are the averaged relative intensities of electrons emitted into the forward hemisphere and $I^{L,b}$ and $I^{R,b}$ those emitted into the backward hemisphere for left- and right-handed circular polarization. In a proof-of-principle experiment, multiphoton PECD-PEPICO was applied to camphor (116) and the following $g_{MP-PECD}$ values were found.

One measurement has been performed with 400 nm femtosecond-laser pulses where two photons excite the 3s-Rydberg state and a third causes ionization. A value for $g_{MP\text{-}PECD}$ of 7.9% has been found. The authors compared this with a theoretical value of 16% and a VUV (single-photon) PECD of −5% (116). There does not exist a comparable two-photon REMPI-CD for camphor, but the situation is very similar to 3-MCP, as the involved intermediate states are mainly due to the carbonyl group. Also in 3-MCP, the 3s-Rydberg state is excited with 400 nm (two-photon excitation) or 200 nm (one-photon excitation) with corresponding g-values of 1.5% and −0.2% (**Figure 5**). Thus, multiphoton-PECD leads to much higher g-values than ECD (one-photon) or two-photon CD in the neutral molecule and even to an enhancement with respect to VUV-PECD (one-photon). Another nice feature of PECD experiments is that they supply information not only about the angular distribution but also the kinetic energy of the emitted electrons. This, on the other hand, is directly correlated to the internal energy of the formed molecular ions (Equation 4). The ion internal energy is relevant if via different neutral intermediate states, different ionic vibrational states are populated due to varying Franck-Condon factors. In other words, differences in multiphoton PECD may be correlated to different intermediate neutral states. This was observed in a second measurement with 380 nm femtosecond-laser pulses. Photoelectrons with a kinetic energy of 0.69 eV (correlated to a vibrationally excited 3s-Rydberg state) revealed a MP-PECD of 5.1%, whereas those with 1.09 eV (correlated to a vibrationless 3p-Rydberg state) revealed an MP-PECD of 3.3%.

In summary, PECD combined with PEPICO and performed with femtosecond-laser pulses is a new, very promising mass-selective method to study molecular chirality. The somewhat unfavorable statistics (due to less than one ionization event per laser pulse) cuts the benefits of exceptionally large g-values (intrinsic to PECD) somewhat. Increasing repetition rates may cope with this problem.

5. SUMMARY AND CONCLUSION

In this review, we presented CD-REMPI together with two other methods to study chirality with mass spectrometric resolution. All three options have their benefits and their drawbacks, which we want to address in closing. The advantage of the diastereomeric approach is that it can be

performed at conventional high-performance mass spectrometers, for example, FTICR (Fourier transform ion cyclotron resonance) or TOF-MS with electrospray or fast atom bombardment ion sources. It is more established than the other two more recent approaches discussed herein, giving rise to many applications. The drawback is that formation of diastereomers is specific to each chiral substance and needs selected chiral partners in each case. In contrast, the other two options (CD-REMPI MS and combined CD-PES & PEPICO) are not restricted in this respect; however, they need minor or major instrument changes of (TOF) mass spectrometers or completely new setups. Their versatility with regard to the number of accessible chemical species is reasonable or even very high; that of CD-REMPI is restricted to g-factors >0.1% and adequate absorption bands, whereas CD-PES is distinguished by an exceptionally large CD effect for all chemical substances. CD-PES & PEPICO is at the stage of proof-of principle experiments. Application to a series of molecules other than camphor will be the next step toward its approval as a general enantiosensitive mass-selective analytical method. Versatility with regard to instrumental combinations is a particular benefit of CD-REMPI. One very promising potential application is its implementation in a laser desorption apparatus for large involatile neutral molecules.

There is much potential for further developments of CD-REMPI MS. For instance, the application of picosecond lasers will supply high repetition rates, high ionization efficiency, low fragmentation rate, and nevertheless sufficient spectral resolution to resolve single vibronic lines, in addition to good handling conditions. This will improve shot-to-shot statistics and, therewith, resolution of asymmetry factors g as well as mass resolution. A further promising approach based on mass-selective CD-absorption spectroscopy is CD-dissociation spectroscopy of molecular ions, including either single-photon absorption into predissociating states (not yet realized) or resonance-enhanced multiphoton absorption into directly dissociating states (CD-REMPD) (first steps have been realized; 72). The latter could be the key to a combined CD-REMPD & MALDI method and thus to the application of mass-selective enantioanalysis to large biomolecules.

This leads us to another fascinating topic, namely, that of chiral molecules on surfaces (see 120, and references therein). It has been found that metal clusters on surfaces show strong size-dependent catalytic effects (121–124). A prerequisite for such studies is the size (i.e., mass)-selective deposition of metal clusters on surfaces (125–129). Very recently, the size-dependent optical response of supported size-selected silver nanoclusters was successfully recorded (130), which is an important step closer to selective photoexcitation. Nonlinear laser spectroscopy on surfaces is a particularly sensitive spectroscopic technique for such studies (131) and, in addition, reveals large enhancement of CD effects (130, 132). It is an ideal analytical tool if one can succeed in depositing not only size- but also enantioselected chiral metal clusters on surfaces as one step toward enantioselective heterogeneous catalysis. CD-REMPI then may serve as the second analytical tool to record the ee of chiral product molecules released from such surfaces. The future may show whether CD-PES and the diastereomeric approach are adequate to solve this task.

DISCLOSURE STATEMENT

The authors are not aware of any affiliations, memberships, funding, or financial holdings that might be perceived as affecting the objectivity of this review.

ACKNOWLEDGMENTS

The authors gratefully acknowledge the fruitful cooperation with Alexander Bornschlegl, Christoph Logé, Martin Thämer, Katharina Titze, Jörn Lepelmeier, and Farinaz Mortaheb, and the support by the German Science Foundation through the projects KA4166/2-1 and BO718/10.

LITERATURE CITED

1. Blaser HU, Spindler F, Studer A. 2001. Enantioselective catalysis in fine chemicals production. *Appl. Catal. Gen.* 221:119–43
2. Yoon TP, Jacobsen EN. 2003. Privileged chiral catalysts. *Science* 299:1691–93
3. Heitbaum M, Glorius F, Escher I. 2006. Asymmetric heterogeneous catalysis. *Angew. Chem. Int. Ed.* 45:4732–62
4. Fales HM, Wright GJ. 1977. Detection of chirality with chemical ionization mass-spectrometer—meso ions in gas-phase. *J. Am. Chem. Soc.* 99:2339–40
5. Baldwin MA, Howell SA, Welham KJ, Winkler FJ. 1988. Identification of chiral isomers by fast atom bombardment mass spectrometry—dialkyl tartrates. *Biomed. Environ. Mass Spectrom.* 16:357–60
6. Sawada M, Shizuma M, Takai Y, Yamada H, Kaneda T, Hanafusa T. 1992. Enantioselectivity in fast-atom bombardment (FAB) mass spectrometry. *J. Am. Chem. Soc.* 114:4405–6
7. Sawada M, Yamaoka H, Takai Y, Kawai Y, Yamada H, et al. 1999. Determination of enantiomeric excess for organic primary amine compounds by chiral recognition fast-atom bombardment mass spectrometry. *Int. J. Mass Spectrom.* 193:123–30
8. Shizuma M, Imamura H, Takai Y, Yamada H, Takeda T, et al. 2000. A new reagent to evaluate optical purity of organic amines by FAB mass spectrometry. *Chem. Lett.* 11:1292–93
9. Sawada M, Takai Y, Imamura H, Yamada H, Takahashi S, et al. 2001. Chiral recognizable host-guest interactions detected by fast-atom bombardment mass spectrometry: application to the enantiomeric excess determination of primary amines. *Eur. J. Mass Spectrom.* 7:447–59
10. Schalley CA. 2001. Molecular recognition and supramolecular chemistry in the gas phase. *Mass Spectrom. Rev.* 20:253–309
11. Shizuma M, Adachi H, Kawamura M, Takai Y, Takeda T, Sawada M. 2001. Chiral discrimination of fructo-oligosaccharides toward amino acid derivatives by induced-fitting chiral recognition. *J. Chem. Soc. Perkin Trans.* 2:592–601
12. Shizuma M, Imamura H, Takai Y, Yamada H, Takeda T, et al. 2001. Facile ee-determination from a single measurement by fast atom bombardment mass spectrometry: a double labeling method. *Int. J. Mass Spectrom.* 210:585–90
13. Shizuma M, Kadoya Y, Takai Y, Imamura H, Yamada H, et al. 2002. New artificial host compounds containing galactose end groups for binding chiral organic amine guests: chiral discrimination and their complex structures. *J. Org. Chem.* 67:4795–807
14. Taji H, Watanabe M, Harada N, Naoki H, Ueda Y. 2002. Diastereomer method for determining ee by 1H NMR and/or MS spectrometry with complete removal of the kinetic resolution effect. *Org. Lett.* 4:2699–702
15. Wu LM, Vogt FG. 2012. A review of recent advances in mass spectrometric methods for gas-phase chiral analysis of pharmaceutical and biological compounds. *J. Pharm. Biomed. Anal.* 69:133–47
16. Awad H, El-Aneed A. 2013. Enantioselectivity of mass spectrometry: challenges and promises. *Mass Spectrom. Rev.* 32:466–83
17. Piovesana S, Samperi R, Lagana A, Bella M. 2013. Determination of enantioselectivity and enantiomeric excess by mass spectrometry in the absence of chiral chromatographic separation: an overview. *Chem. Eur. J.* 19:11478–94
18. Vékey K, Czira G. 1997. Distinction of amino acid enantiomers based on the basicity of their dimers. *Anal. Chem.* 69:1700–5
19. Cooks RG, Kruger TL. 1977. Intrinsic basicity determination using metastable ions. *J. Am. Chem. Soc.* 99:1279–81
20. Tao WA, Zhang DX, Wang F, Thomas PD, Cooks RG. 1999. Kinetic resolution of D, L-amino acids based on gas-phase dissociation of copper(II) complexes. *Anal. Chem.* 71:4427–29
21. Duxi Z, Tao WA, Cooks RG. 2001. Chiral resolution of D- and L-amino acids by tandem mass spectrometry of Ni(II)-bound trimeric complexes. *Int. J. Mass Spectrom.* 204:159–69
22. Wu LM, Clark RL, Cooks RG. 2003. Chiral quantification of D-, L-, and meso-tartaric acid mixtures using a mass spectrometric kinetic method. *Chem. Commun.* 9:136–37

23. Wu LM, Cooks RG. 2003. Chiral analysis using the kinetic method with optimized fixed ligands: applications to some antibiotics. *Anal. Chem.* 75:678–84
24. Bagheri H, Chen H, Cooks RG. 2004. Chiral recognition by proton transfer reactions with optically active amines and alcohols. *Chem. Commun.* 23:2740–41
25. Wu LM, Cooks G. 2005. Chiral and isomeric analysis by electrospray ionization and sonic spray ionization using the fixed-ligand kinetic method. *Eur. J. Mass Spectrom.* 11:231–42
26. Young BL, Cooks RG. 2007. Improvements in quantitative chiral determinations using the mass spectrometric kinetic method. *Int. J. Mass Spectrom.* 267:199–204
27. Tao WA, Clark RL, Cooks RG. 2002. Quotient ratio method for quantitative enantiomeric determination by mass spectrometry. *Anal. Chem.* 74:3783–89
28. Tao WA, Cooks RG, Nikolaev EN. 2002. Chiral preferences in the dissociation of homogeneous amino acid/metal ion clusters. *Eur. J. Mass Spectrom.* 8:107–15
29. Wu L, Tao WA, Cooks RG, Begley JA, Lampert B. 2002. Improved accuracy in quantitative analysis of chiral drugs using a ratio of ratio of ratio's (RRR's) kinetic method treatment. *Abstr. Pap. Am. Chem. Soc.* 224:163
30. Wu LM, Tao WA, Cooks RG. 2003. Kinetic method for the simultaneous chiral analysis of different amino acids in mixtures. *J. Mass Spectrom.* 38:386–93
31. Alrabaa AR, Breheret E, Lahmani F, Zehnacker A. 1995. Enantiodifferentiation in jet-cooled van-der-waals complexes of chiral molecules. *Chem. Phys. Lett.* 237:480–84
32. Pierini M, Troiani A, Speranza M, Piccirillo S, Bosman C, et al. 1997. Gas-phase enantiodifferentiation of chiral molecules: chiral recognition of 1-phenyl-1-propanol/2-butanol clusters by resonance enhanced multiphoton ionization spectroscopy. *Angew. Chem. Int. Ed.* 36:1729–31
33. Latini A, Toja D, Giardini-Guidoni A, Palleschi A, Piccirillo S, Speranza M. 1999. Spectroscopic enantiodifferentiation of chiral molecules in the gas phase. *Chirality* 11:376–80
34. Filippi A, Giardini A, Piccirillo S, Speranza M. 2000. Gas-phase enantioselectivity. *Int. J. Mass Spectrom.* 198:137–63
35. Guidoni AG, Latini A, Satta M, Piccirillo S, Di Palma TM. 2000. Laser spectroscopy of clusters—application to differentiation of chiral systems. *Synth. Metals* 115:279–82
36. Guidoni AG, Piccirillo S, Scuderi D, Satta M, Di Palma TM, et al. 2001. Photochemical R2PI study of chirality and intermolecular forces in supersonic beam. *Int. J. Photoenergy* 3:223–27
37. Scuderi D, Paladini A, Satta M, Catone D, Piccirillo S, et al. 2002. Chiral aggregates of indan-1-ol with secondary alcohols and water: laser spectroscopy in supersonic beams. *Phys. Chem. Chem. Phys.* 4:4999–5003
38. Guidoni AG, Piccirillo S, Scuderi D, Satta M, Filippi A, et al. 2003. Laser studies of chiral molecules. In *Laser Processing of Advanced Materials and Laser Microtechnologies*, ed. FH Dausinger, VI Konov, VY Baranov, VY Panchenko, pp. 42–47. Bellingham, WA: Soc. Opt. Eng.
39. Scuderi D, Paladini A, Satta M, Catone D, Filippi A, et al. 2003. Gas-phase complexes: noncovalent interactions and stereospecificity. *Int. J. Mass Spectrom.* 223:159–68
40. Speranza M. 2004. Chiral clusters in the gas phase. In *Advances in Physical Organic Chemistry*, Vol. 39, ed. JP Richard, pp. 147–281. San Diego: Academic
41. Speranza M, Satta M, Piccirillo S, Rondino F, Paladini A, et al. 2005. Chiral recognition by mass-resolved laser spectroscopy. *Mass Spectrom. Rev.* 24:588–610
42. Giardini A, Rondino F, Paladini A, Hortal AR, Satta M, et al. 2008. Monosolvation effects in chiral fluoroorganic compounds: an R2PI study. *Phys. Scr.* 78:058121
43. Speranza M, Rondino F, Satta M, Paladini A, Giardini A, et al. 2009. Molecular and supramolecular chirality: R2PI spectroscopy as a tool for the gas-phase recognition of chiral systems of biological interest. *Chirality* 21:119–44
44. Rondino F, Paladini A, Ciavardini A, Casavola A, Catone D, et al. 2011. Chiral recognition between 1-(4-fluorophenyl)ethanol and 2-butanol: higher binding energy of homochiral complexes in the gas phase. *Phys. Chem. Chem. Phys.* 13:818–24
45. Berova N, Nakanishi K, Woody RW. 2000. *Circular Dichroism*: *Principles and Applications*. New York: Wiley-VCH. 2nd ed.

46. Boesl U. 1991. Multiphoton excitation and mass-selective ion detection for neutral and ion spectroscopy. *J. Phys. Chem.* 95:2949–62
47. Walter K, Boesl U, Schlag EW. 1989. Molecular ion spectroscopy - resonance-enhanced multiphoton dissociation spectra of the fluorobenzene cation. *Chem. Phys. Lett.* 162:261–68
48. Walter K, Weinkauf R, Boesl U, Schlag EW. 1988. Molecular ion spectroscopy—mass selected, resonant 2-photon dissociation spectra of CH3I+ and CD3I+. *J. Chem. Phys.* 89:1914–22
49. Boesl U, Neusser HJ, Schlag EW. 1979. Spectra of individual molecular isotopes in an unseparated natural mixture. *Chem. Phys. Lett.* 61:57–61
50. Oser H, Coggiola MJ, Young SE, Crosley DR, Hafer V, Grist G. 2007. Membrane introduction/laser photoionization time-of-flight mass spectrometry. *Chemosphere* 67:1701–8
51. Schiewek R, Schellentrager M, Monnikes R, Lorenz M, Giese R, et al. 2007. Ultrasensitive determination of polycyclic aromatic compounds with atmospheric-pressure laser ionization as an interface for GC/MS. *Anal. Chem.* 79:4135–40
52. Misawa K, Matsumoto J, Yamato Y, Mae S, Ishiuchi S, et al. 2008. *Real-time and direct measurement of pollutants in exhaust gas utilizing supersonic jet/ resonance enhanced multi-photon ionization*. Tech. Pap. 2008-01-0761, SAE Int., Warrendale, PA
53. Boesl U, Weishaeupl R, Thiel W, Püffel P, Frey R. 2005. *Time-resolved chemical analysis by laser mass spectrometry: monitoring of in-cylinder and catalytic-converter processes of combustion engines*. Tech. Pap. 2005-01-0679, SAE Int., Warrendale, PA
54. Bente M, Sklorz M, Streibel T, Zimmermann R. 2008. Online laser desorption-multiphoton postionization mass spectrometry of individual aerosol particles: molecular source indicators for particles emitted from different traffic-related and wood combustion sources. *Anal. Chem.* 80:8991–9004
55. Boesl U, Heger H-J, Zimmermann R, Püffel P, Nagel H. 2000. Laser mass spectrometry in trace analysis. In *Encyclopedia of Chemical Analysis*, ed. RA Meyers, pp. 2087–118. Chichester, UK: John Wiley & Sons
56. Li R, Sullivan R, Al-Basheer W, Pagni RM, Compton RN. 2006. Linear and nonlinear circular dichroism of R-(+)-3-methylcyclopentanone. *J. Chem. Phys.* 125:144304
57. Peticola Wl. 1967. Multiphoton spectroscopy. *Annu. Rev. Phys. Chem.* 18:233–60
58. McClain WM. 1974. Two-photon molecular spectroscopy. *Acc. Chem. Res.* 7:129–35
59. Tinoco I Jr. 1975. 2-Photon circular-dichroism. *J. Chem. Phys.* 62:1006–9
60. Power EA. 1975. 2-Photon circular-dichroism. *J. Chem. Phys.* 63:1348–50
61. Gunde KE, Burdicka GW, Richardson FS. 1996. Chirality-dependent two-photon absorption probabilities and circular dichroic line strengths: theory, calculation and measurement. *Chem. Phys.* 208:195–219
62. Rizzo A, Lin N, Ruud K. 2008. Ab initio study of the one- and two-photon circular dichroism of R-(+)-3-methyl-cyclopentanone. *J. Chem. Phys.* 128:164312
63. Lin N, Santoro F, Rizzo A, Luo Y, Zhao X, Barone V. 2009. Theory for vibrationally resolved two-photon circular dichroism spectra. Application to (R)-(+)-3-methylcyclopentanone. *J. Phys. Chem. A* 113:4198–207
64. Boesl von Grafenstein U, Bornschlegl A. 2006. Circular dichroism laser mass spectrometry: differentiation of 3-methylcyclopentanone enantiomers. *ChemPhysChem* 7:2085–87
65. Bornschlegl A, Loge C, Boesl U. 2007. Investigation of CD effects in the multi photon ionisation of R-(+)-3-methylcyclopentanone. *Chem. Phys. Lett.* 447:187–91
66. Breunig HG, Urbasch G, Horsch P, Cordes J, Koert U, Weitzel K-M. 2009. Circular dichroism in ion yields of femtosecond-laser mass spectrometry. *ChemPhysChem* 10:1199–202
67. Horsch P, Urbasch G, Weitzel KM. 2011. Circular dichroism in ion yields in multiphoton ionization of (R)-propylene oxide employing femtosecond laser pulses. *Z. Phys. Chem.-Int. J. Res. Phys. Chem. Chem. Phys.* 225:587–94
68. Horsch P, Urbasch G, Weitzel KM, Kroner D. 2011. Circular dichroism in ion yields employing femtosecond laser ionization—the role of laser pulse duration. *Phys. Chem. Chem. Phys.* 13:2378–86
69. Horsch P, Urbasch G, Weitzel K-M. 2012. Analysis of chirality by femtosecond laser ionization mass spectrometry. *Chirality* 24:684–90
70. Lux C, Liang Q, Sarpe-Tudoran C, Wollenhaupt M, Baumert T. 2010. Fragmentation studies of chiral molecules via femtosecond-laser mass spectrometry. Presented at Annu. Conf. Deutsche Physikalische Gesellschaft, Mar. 9, Hannover, Ger.

71. Logé C, Boesl U. 2012. Laser mass spectrometry with circularly polarized light: two-photon circular dichroism. *Phys. Chem. Chem. Phys.* 14:11981–89
72. Logé C, Boesl U. 2012. Laser mass spectrometry with circularly polarized light: circular dichroism of molecular ions. *ChemPhysChem* 13:4218–23
73. Kröner D. 2015. Laser-driven electron dynamics for circular dichroism in mass spectrometry: from one-photon excitations to multiphoton ionization. *Phys. Chem. Chem. Phys*. 17:19643–55
74. Kröner D, Shibl MF, González L. 2003. Asymmetric laser excitation in chiral molecules: quantum simulations for a proposed experiment. *Chem. Phys. Lett*. 372(1–2):242–48
75. Logé C, Bornschlegi A, Boesl U. 2009. Twin mass peak ion source for comparative mass spectrometry: application to circular dichroism laser MS. *Int. J. Mass Spectrom.* 281:134–39
76. Loge C, Boesl U. 2011. Multiphoton ionization and circular dichroism: new experimental approach and application to natural products. *ChemPhysChem* 12:1940–47
77. Wiley WC, McLaren IH. 1955. Time-of-flight mass spectrometer with improved resolution. *Rev. Sci. Instrum.* 26:1150–57
78. Mamyrin BA, Karataev VI, Shmikk DV, Zagulin VA. 1973. The mass-reflectron, a new non-magnetic time-of-flight mass spectrometer with high resolution. *Sov. Phys.J. Exp. Theor. Phys.* 37:45–48
79. Boesl U, Weinkauf R, Schlag EW. 1992. Reflectron time-of-flight mass-spectrometry and laser excitation for the analysis of neutrals, ionized molecules and secondary fragments. *Int. J. Mass Spectrom. Ion Process.* 112:121–66
80. Boesl U, Bornschlegl A, Loge C, Titze K. 2013. Resonance-enhanced multiphoton ionization with circularly polarized light: chiral carbonyls. *Anal. Bioanal. Chem.* 405:6913–24
81. Brint P, Meshulam E, Gedanken A. 1984. Excited electronic states of limonene: a circular dichroism and photoelectron spectroscopy study of d-limonene. *Chem. Phys. Lett.* 109:383–87
82. Macleod NA, Butz P, Simons JP, Grant GH, Baker CM, Tranter GE. 2004. Electronic circular dichroism spectroscopy of 1-(R)-phenylethanol: the "sector rule" revisited and an exploration of solvent effects. *Isr. J. Chem.* 44:27–36
83. Macleod NA, Butz P, Simons JP, Grant GH, Baker CM, Tranter GE. 2005. Structure, electronic circular dichroism and Raman optical activity in the gas phase and in solution: a computational and experimental investigation. *Phys. Chem. Chem. Phys.* 7:1432–40
84. Pickard ST, Smith HE. 1990. Optically-active amines. 34. Application of the benzene chirality rule to ring-substituted phenylcarbinamines and carbinols. *J. Am. Chem. Soc.* 112:5741–47
85. Naguleswaran S, Reid MF, Stedman GE. 2000. Prediction of pure electric-dipole two-photon absorption circular dichroism in lanthanide compounds. *Chem. Phys.* 256:207–12
86. Dekkers HPJM, Closs LE. 1976. The optical activity of low-symmetry ketones in absorption and emission. *J. Am. Chem. Soc.* 98:2210–19
87. Titze K, Zollitsch T, Heiz U, Boesl U. 2014. Laser mass spectrometry with circularly polarized light: circular dichroism of cold molecules in a supersonic gas beam. *ChemPhysChem* 15:2762–67
88. Smalley RE, Wharton L, Levy DH. 1977. Molecular optical spectroscopy with supersonic beams and jets. *Acc. Chem. Res.* 10:139–45
89. Duncan MA, Dietz TG, Smalley RE. 1979. Efficient multi-photon ionization of metal-carbonyls cooled in a pulsed supersonic beam. *Chem. Phys.* 44:415–19
90. Lubman DM. 1987. Optically selective molecular mass spectrometry. *Anal. Chem.* 59:31A–40A
91. Weickhardt C, Zimmermann R, Boesl U, Schlag EW. 1993. Laser mass-spectrometry of dibenzodioxin dibenzofuran and 2 isomers of dichlorodibenzodioxins—selective ionization. *Rapid Commun. Mass Spectrom.* 7:183–85
92. Zimmermann R, Lermer C, Schramm KW, Kettrup A, Boesl U. 1995. 3-Dimensional trace analysis—combination of gas-chromatography, supersonic beam UV spectroscopy and time-of-flight mass-spectrometry. *Eur. Mass Spectrom.* 1:341–51
93. Hong A, Choi CM, Eun HJ, Jeong C, Heo J, Kim NJ. 2014. Conformation-specific circular dichroism spectroscopy of cold, isolated chiral molecules. *Angew. Chem. Int. Ed.* 53:7805–8
94. Zhang J, Chiang WY, Laane J. 1993. Jet-cooled fluorescence excitation-spectra, conformation, and carbonyl wagging potential-energy function of cyclopentanone and its deuterated isotopomers in the S_1 (*n*, PI-asterisk) electronic excited-states. *J. Chem. Phys.* 98:6129–37

95. Dierksen M, Grimme S. 2006. A theoretical study of the chiroptical properties of molecules with isotopically engendered chirality. *J. Chem. Phys.* 124:174301
96. Na L, Santoro F, Xian Z, Rizzo A, Barone V. 2008. Vibronically resolved electronic circular dichroism spectra of (R)-(+)-3-methylcyclopentanone: a theoretical study. *J. Phys. Chem. A* 112:12401–11
97. Na L, Yi L, Santoro F, Xian Z, Rizzo A. 2008. Vibronically-induced change in the chiral response of molecules revealed by electronic circular dichroism spectroscopy. *Chem. Phys. Lett.* 464:144–49
98. Ritchie B. 1976. Theory of angular-distribution of photoelectrons ejected from optically active molecules and molecular negative-ions. *Phys. Rev. A* 13:1411–15
99. Powis I. 2000. Photoelectron spectroscopy and circular dichroism in chiral biomolecules: L-alanine. *J. Phys. Chem. A* 104:878–82
100. Bowering N, Lischke T, Schmidtke B, Muller N, Khalil T, Heinzmann U. 2001. Asymmetry in photoelectron emission from chiral molecules induced by circularly polarized light. *Phys. Rev. Lett.* 86:1187–90
101. Hergenhahn U, Rennie EE, Kugeler O, Marburger S, Lischke T, et al. 2004. Photoelectron circular dichroism in core level ionization of randomly oriented pure enantiomers of the chiral molecule camphor. *J. Chem. Phys.* 120:4553–56
102. Nahon L, Garcia GA, Harding CJ, Mikajlo E, Powis I. 2006. Determination of chiral asymmetries in the valence photoionization of camphor enantiomers by photoelectron imaging using tunable circularly polarized light. *J. Chem. Phys.* 125:114309
103. Powis I. 2008. Photoelectron circular dichrosim in chiral molecules. In *Advances in Chemical Physics*, ed. JC Light, pp. 267–329. New York: Wiley
104. Nahon L, Powis I. 2010. Valence photoelectron circular dichroism of gas phase enantiomers. In *Chiral Recognition in the Gas Phase*, ed. A Zehnacker, pp. 1–26. Boca Raton, FL: CRC
105. Powis I. 2012. Photoelectron circular dichroism. In *Comprehensive Chiroptical Spectroscopy*, ed. N Berova, PL Polavarapu, K Nakanishi, RW Woody, pp. 407–31. New York: Wiley
106. Lux C, Wollenhaupt M, Bolze T, Liang QQ, Kohler J, et al. 2012. Circular dichroism in the photoelectron angular distributions of camphor and fenchone from multiphoton ionization with femtosecond laser pulses. *Angew. Chem. Int. Ed.* 51:5001–5
107. Lux C, Wollenhaupt M, Sarpe C, Baumert T. 2015. Photoelectron circular dichroism of bicyclic ketones from multiphoton ionization with femtosecond laser pulses. *ChemPhysChem* 16:115–37
108. Baer T, Weitzel KM, Booze J. 1991. Photoelectron photoion coincidence studies of ion dissociation dynamics. In *Vacuum Ultraviolet Photoionization and Photodissociation of Molecules and Clusters*, ed. C-Y Ng, pp. 259–96. Singapore: World Sci.
109. Brehm B, von Puttkamer E. 1967. Koinzidenzmessung von photoionen und photoelektronen bei methan. *Z. Naturforsch. A* 22:8–10
110. Davies JA, LeClaire JE, Continetti RE, Hayden CC. 1999. Femtosecond time-resolved photoelectron-photoion coincidence imaging studies of dissociation dynamics. *J. Chem. Phys.* 111:1–4
111. Davies JA, Continetti RE, Chandler DW, Hayden CC. 2000. Femtosecond time-resolved photoelectron angular distributions probed during photodissociation of NO_2. *Phys. Rev. Lett.* 84:5983–86
112. Continetti RE, Hayden CC. 2004. Coincidence imaging techniques. In *Modern Trends in Reaction Dynamics*, ed. X Yang, K Liu, pp. 475–528. Singapore: World Sci.
113. Rijs AM, Janssen MHM, Chrysostom ETH, Hayden CC. 2004. Femtosecond coincidence imaging of multichannel multiphoton dynamics. *Phys. Rev. Lett.* 92:123002
114. Vredenborg A, Roeterdink WG, Janssen MHM. 2008. A photoelectron-photoion coincidence imaging apparatus for femtosecond time-resolved molecular dynamics with electron time-of-flight resolution of sigma = 18 ps and energy resolution Delta E/E = 3.5%. *Rev. Sci. Instrum.* 79:063108
115. Vredenborg A, Lehmann CS, Irimia D, Roeterdink WG, Janssen MHM. 2011. The reaction microscope: imaging and pulse shaping control in photodynamics. *ChemPhysChem* 12:1459–73
116. Lehmann CS, Ram NB, Powis I, Janssen MHM. 2013. Imaging photoelectron circular dichroism of chiral molecules by femtosecond multiphoton coincidence detection. *J. Chem. Phys.* 139:234307
117. Ram NB, Lehmann CS, Janssen MHM. 2013. Probing chirality with a femtosecond reaction microscope. *EPJ Web Conf.* 41:02029
118. Janssen MHM, Powis I. 2014. Detecting chirality in molecules by imaging photoelectron circular dichroism. *Phys. Chem. Chem. Phys.* 16:856–71

119. Lehmann CS, Ram NB, Janssen MHM. 2012. Velocity map photoelectron-photoion coincidence imaging on a single detector. *Rev. Sci. Instrum.* 83:093103
120. Heister P, Luenskens T, Thaemer M, Kartouzian A, Gerlach S, et al. 2014. Orientational changes of supported chiral 2,2′-dihydroxy-1,1′-binaphthyl molecules. *Phys. Chem. Chem. Phys.* 16:7299–306
121. Harding C, Habibpour V, Kunz S, Farnbacher AN-S, Heiz U, et al. 2009. Control and manipulation of gold nanocatalysis: effects of metal oxide support thickness and composition. *J. Am. Chem. Soc.* 131:538–48
122. Roettgen MA, Abbet S, Judai K, Antonietti J-M, Woerz AS, et al. 2007. Cluster chemistry: size-dependent reactivity induced by reverse spill-over. *J. Am. Chem. Soc.* 129:9635–39
123. Schweinberger FF, Berr MJ, Doeblinger M, Wolff C, Sanwald KE, et al. 2013. Cluster size effects in the photocatalytic hydrogen evolution reaction. *J. Am. Chem. Soc.* 135:13262–65
124. Tang X, Bumueller D, Lim A, Schneider J, Heiz U, et al. 2014. Catalytic dehydration of 2-propanol by size-selected $(WO_3)_n$ and $(MoO_3)_n$ metal oxide clusters. *J. Phys. Chem. C* 118:29278–86
125. Heiz U, Vayloyan A, Schumacher E. 1997. A new cluster source for the generation of binary metal clusters. *Rev. Sci. Instrum.* 68:3718–22
126. Heiz U. 1998. Physical and chemical properties of size-selected, supported clusters. In *Recent Research Developments in Physical Chemistry*, Vol. 2, Part II, ed. SG Pandalai, pp. 1029–86. Trivandrum, India: Transw. Res. Netw.
127. Gilb S, Hartl K, Kartouzian A, Peter J, Heiz U, et al. 2007. Cavity ring-down spectroscopy of metallic gold nanoparticles. *Eur. Phys. J. D* 45:501–6
128. Kartouzian A, Thaemer M, Soini T, Peter J, Pitschi P, et al. 2008. Cavity ring-down spectrometer for measuring the optical response of supported size-selected clusters and surface defects in ultrahigh vacuum. *J. Appl. Phys.* 104:124313
129. Kartouzian A, Thaemer M, Heiz U. 2010. Characterisation and cleaning of oxide support materials for cavity ring-down spectroscopy. *Phys. Stat. Solidi B* 247:1147–51
130. Lunskens T, Heister P, Thamer M, Walenta CA, Kartouzian A, Heiz U. 2015. Plasmons in supported size-selected silver nanoclusters. *Phys. Chem. Chem. Phys.* 17:17541–44
131. Thaemer M, Kartouzian A, Heister P, Gerlach S, Tschurl M, et al. 2012. Linear and nonlinear laser spectroscopy of surface adsorbates with sub-monolayer sensitivity. *J. Phys. Chem. C* 116:8642–48
132. Fischer P, Hache F. 2005. Nonlinear optical spectroscopy of chiral molecules. *Chirality* 17:421–37
133. Loge C, Bornschegl A, Boesl U. 2009. Progress in circular dichroism laser mass spectrometry. *Anal. Bioanal. Chem.* 395:1631